USE OF ENTRY VEHICLE RESPONSES TO DEFINE THE PROPERTIES OF THE MARS ATMOSPHERE

Alvin Seiff* and David E. Reese, Jr.+

The principles by which the atmospheric properties of an unknown planetary atmosphere can be deduced from responses of a probe vehicle entering the atmosphere are developed. Experiments to determine atmospheric density and pressure as functions of altitude, and to detect and determine quantities of selected gases in the atmosphere are examined in detail. Accuracies and experiment problem areas are treated.

The atmospheric density and pressure may be determined with very good accuracy during hypersonic flight, from altitudes of several hundred thousand feet to ground level, by measurement of three components of vehicle acceleration supplemented in the terminal phase by measurements of pitot and static pressure and atmospheric temperature. The accuracy, ease of data analysis, and minimization of total data quantity are all favorably affected by choice of probe configurations which do not develop lift and which have drag coefficient independent of Mach number, Reynolds number, gas composition, and angle of attack. These considerations strongly suggest that the probe geometry should be spherical. Other geometries having approximately the aerodynamic properties desired are discussed.

The approach to the detection of atmospheric species is by spectrometry of selected wave lengths of emission from the hot atmospheric gases in the shock layer. Laboratory studies and theory have shown that very bright emission behind the bow wave in atmospheres of nitrogen and carbon dioxide is associated with the cyanogen radical, and detection of the violet band system would constitute direct evidence for nitrogen in the atmosphere. The quantity can be deduced. Other radiometers to measure the nitric oxide and argon radiations are dicussed.

*Chief, Vehicle Environment Division, National Aeronautics and Space Administration, Ames Research Center, Moffett Field, California

+Assistant Chief, Vehicle Environment Division, National Aeronautics and Space Administration, Ames Research Center, Moffett Field, California

INTRODUCTION

The use of entry vehicle responses for measuring the properties of planetary atmospheres provides measurement techniques that are both direct and simple, permits the study of upper atmospheric properties as well as low level properties, and does not require parachute deployment or landing survival to succeed.[1] A study of this approach to the exploration of the Mars atmosphere has indicated that use of accelerometers, pressure and temperature sensors, and narrow band radiometers in a spherical probe can provide much useful information on the structure and composition of the atmosphere.[2] The present paper will extend the discussion of these experiments to present more completely the underlying basis, the difficulties, and the accuracy analysis. Emphasis is on the atmosphere of Mars.

MEASUREMENTS OF ALTITUDE PROFILES OF ATMOSPHERIC DENSITY, PRESSURE, AND TEMPERATURE

It will be useful for the later discussion to review the principles of atmospheric measurements from a probe entering the atmosphere at speeds that are high compared to the speed of sound, and to establish the kinds of measurements that are and are not most useful. The vehicle is enveloped by a shock layer in which the state properties have been considerably altered from ambient values. The pressure and temperature in this layer may be represented by*

$$p = p_\infty + P\rho_\infty V_\infty^2/2 \tag{1}$$

$$\bar{h} = \int_0^T c_p \, dT \approx c_p T_\infty + (V_\infty^2/2)(1 - \cos^2 \delta) \tag{2}$$

from which the terms introducing difference between ambient (sub ∞) and shock layer (no subscript) properties may be identified. In Eq. (1), e.g., the second term on the right is the difference $p - p_\infty$, which, at high flight speeds, is normally large compared to p_∞. It may be considered either as a correction to the measured pressure for obtaining the ambient pressure or (more profitably if p_∞ is negligible compared to p) the measured pressure may be considered a direct measure of the atmospheric density. The pressure coefficient P is of the order of 1 for blunt bodies, and even for sharp-nosed slender bodies, where P may be close to 0, the variations in the correction term due to angle of attack, Mach number, Reynolds number, and gas composition can be large compared to the ambient pressure. Hence, measurements of pressure in the shock layer are inherently not descriptive of the ambient pressure, depending instead sensitively on the aerodynamics (coefficient P) and the velocity.

Similarly, the difference between the measured enthalpy and the ambient enthalpy, $\bar{h} - \bar{h}_\infty$, is proportional to V_∞^2, and, at the high speeds characteristic of planetary entry, is large compared to $\bar{h}_\infty$. This is true even for slender bodies ($\delta = 0$) if they have blunted tips, a case for which Eq. (2) fails to estimate the temperature closely. Most important, however, the temperature measured either on the insulated vehicle surface or on a sensor projecting into the flow is approximately the flow total temperature,

*Notation is given at end of paper.

given by setting $\delta = 90^\circ$ in Eq. (2). These temperatures are very large compared to ambient and provide a poor basis for estimating ambient values. Thus, it is clear that measuring the state properties of gas in the shock layer is not an attractive way of studying the undisturbed atmosphere from a hypersonic probe vehicle. This is a well-known fact of long standing among high speed aerodynamicists and those who have made measurements of the Earth's upper atmosphere from high speed vehicles.

The vehicle deceleration, however, provides a direct and accurate basis for measuring ambient density and pressure, if properly applied. The familiar relationship between gasdynamic drag and ambient density

$$D = C_D(1/2\rho_\infty V_\infty^2 A) \tag{3}$$

plus Newton's second law of motion

$$D = -ma_S \tag{4}$$

lead to the equation for density

$$\rho_\infty = -2(m/C_D A)(a_S/V_\infty^2) . \tag{5}$$

A basic difference between Eqs. (1) and (5) is that in Eq. (1) the quantity measured is subject to a large correction to obtain the quantity desired, whereas in Eq. (5), the quantity measured (acceleration) is directly proportional to the quantity desired. This equation has been used as the basis for accurate measurements of the density of the Earth's upper atmosphere.[3,4]

The ambient pressure may be obtained by integrating the density to obtain the weight of the atmosphere from altitude h to the upper altitude limit of the sensible atmosphere

$$p_\infty = \int_h^\infty \rho g \, dh \tag{6}$$

and the RT_∞ product of the atmosphere is then known from the gas law

$$RT_\infty = p_\infty/\rho_\infty \tag{7}$$

Given the molecular weight of the atmospheric gases, the temperature also becomes known.

To obtain the ambient density from Eq. (5), however, one must know the vehicle mass m, frontal area A, drag coefficient C_D, and velocity V_∞ at the instant of measurement, and must also be able to distinguish between the drag acceleration and that component of acceleration which is due to lift, since the entry body will in general experience oscillations in angle of attack. The mass and area are known exactly, except for ablation effects which are minor and can be estimated for speeds of entry into the near planets. The other three factors merit discussion.

The drag coefficient must be considered a function of four of the entry variables, the Mach number, the Reynolds number, the gas composition, and the angle of attack. For the general case, then, these four variables must be defined at every instant of measurement to permit the definition of density by Eq. (5). One can also imagine an ideal case in which C_D is independent of these variables. While a perfect independence of Mach number, Reynolds number, and gas composition cannot be realized, blunt low-fineness-ratio bodies in the supersonic-hypersonic speed range have dimensionless pressure distributions which are nearly independent of Mach number and also have little viscous drag and therefore little dependence on Reynolds number (Figs. 1 and 2).[5-9] They are, in addition, relatively insensitive to gas composition[10,11] (Fig. 3). The use of such bodies in density measurements is of advantage,

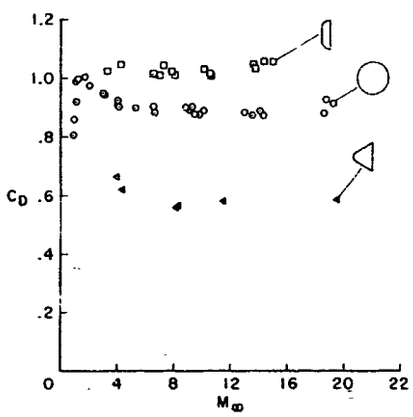

Fig. 1 Insensitivity to Mach Number of the Drag Coefficients of High Drag Bodies

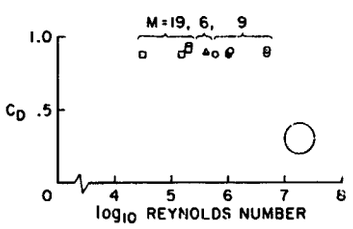

Fig. 2 Insensitivity to Reynolds Number of the Drag Coefficient of a Sphere at Supersonic Speeds

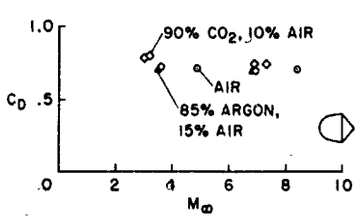

Fig. 3 Gas Composition Effect on the Drag Coefficient of a High Drag Body

since it improves the precision of the density and relaxes the necessity for iterative data reduction and accurate supplementary information. In contrast, C_D is considerably more variable for slender bodies, the sensitivity to Mach number and angle of attack being typically as shown in Fig. 4. The data in Figs. 1-4 include some previously unpublished measurements by B. J. Short, J. Terry, D. Kirk, and P. Intrieri of Ames Research Center along with data from the references cited.

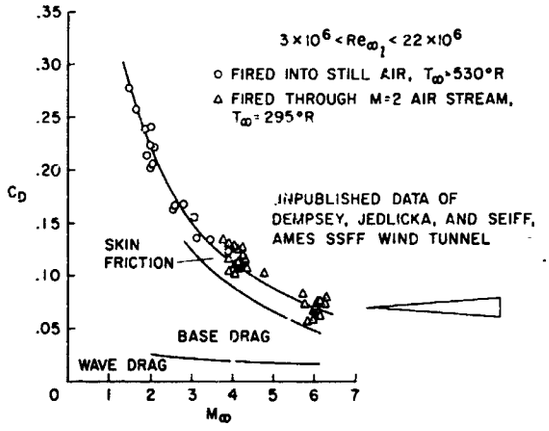

(a) Mach Number

Fig. 4 Effects of Mach Number and Angle of Attack on Drag Coefficient of Slender Bodies

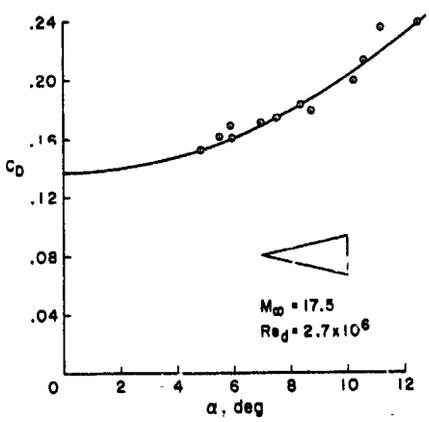

(b) Angle of Attack

Fig. 4 Concluded

Invariance of drag coefficient with angle of attack is a special property, possessed perfectly by only one configuration, the sphere. However, it can be found approximately in configurations having zero lift curve slope, since to a good order of approximation, the coefficient of drag increase with angle of attack is the lift curve slope.

$$C_D = C_{D_{\alpha=0}} + C_{L_\alpha}\alpha^2 \tag{8}$$

An example of such a configuration is the cone of 45° half-angle, or the round-nosed cone of about the same half-angle. At large angles of attack, variations in C_D will occur, since the lift curve slope does not remain zero for all attitudes. Those configurations having C_D nearly independent of attitude will greatly simplify the measurement and data reduction problems.

For bodies which develop lift, resolution of the accelerations is needed to interpret the data. Thus, in the sketch, the body axis (x axis) is at an

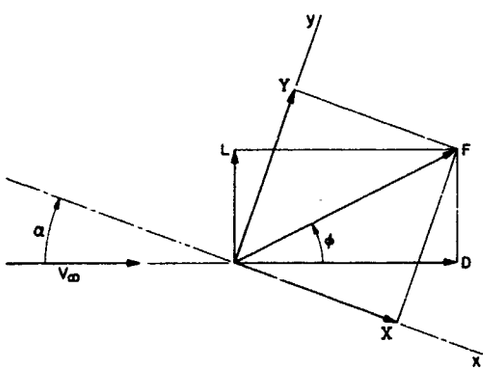

Sketch (a)

angle α relative to the flight or wind direction leading to a lift force L in addition to the drag D, their resultant being F. The resultant acceleration is resolved by accelerometers on the center of gravity into components normal to the body axis a_y and along the body axis a_x. The angle of attack is unknown except as it is defined by the accelerometer data, and it can be shown that

$$\alpha = \tan^{-1} a_y/a_x - \tan^{-1} L/D \tag{9}$$

where a_y and a_x are the acceleration components along the body-fixed y and x axes, and the angle whose tangent is L/D has been designated φ in the sketch. The angle φ is a function of the angle of attack $\varphi = \tan^{-1} L/D = \varphi(\alpha)$ and the functional relationship may be defined by wind-tunnel measurements. This function may vary with Mach number, Reynolds number, and gas composition. When angle of attack is established, the desired drag acceleration is obtained from

$$a_s = a_x \cos \alpha + a_y \sin \alpha \tag{10}$$

Alternatively, one could analyze the data in terms of the resultant acceleration, replacing C_D by C_F in Eq. (5), and a_s by a_F. Equation (9) is still needed to define α, since C_F is generally a strong function of α. With configurations developing no lift, considerable simplification is realized; Eq. (9) reduced to $\tan \alpha = a_y/a_x$, and no wind-tunnel data are used in the analysis. These equations have, for simplicity, been written for two dimensions, but are readily generalizable to three.

The definition of velocity for every instant of measurement remains to be considered. Three approaches will be discussed, and in an actual case, all three could be used in supplementary fashion. Since the accelerometers needed for determining the density are available, it is possible to integrate the pathwise (drag) component over time to track the velocity. The velocity at entry is known from tracking the trajectory through interplanetary space, and the velocity equation after entry is

$$V = V_E + \int_o^t a_s \, dt \tag{11}$$

where a_s is negative. While this approach would seem to be completely adequate, the accuracy must be considered when V becomes small compared to V_E. The velocity is then the small difference between two nearly equal numbers, V_E and the integral. Errors in the integral must be limited to the level of acceptable errors in the velocity. This will be illustrated subsequently in its effect on the density determination.

Other approaches to measuring velocity are by Doppler tracking of the entry probe from its radio communication signal, and airspeed indication by pitot and static pressure measurements. The former has two problems associated with it. One is the radio communication blackout, during which no information is obtained. This means that Doppler tracking cannot be used to do the precise and continuous definition of atmospheric density considered herein. It has been shown, however, that with interpolation techniques to cover the period of blackout, the complete atmosphere can be defined with relatively good success by means of Doppler data alone if it is sufficiently accurate.[12] The Doppler information is obtained primarily before entry and after the velocity has dropped below about 10,000 ft/sec. Thus, it is a useful supplement to the accelerometer data which lose accuracy at the lower speeds. The other problem of the Doppler measurement is that it gives only the component of velocity along the line of communication. The complete motion must therefore be synthesized from the data in a trajectory analysis.

Pitot and static pressure measurements can be used to indicate the velocity below sonic speed precisely where it is most important to supplement the accelerometer velocity data. For low speed incompressible flow, Bernoulli's principle provides the well-known basis for determining velocity from pitot and static pressure measurements:

$$q_\infty = 1/2 \rho_\infty V_\infty^2 = p_t - p_\infty \tag{12}$$

With the gas law, this equation is solved for velocity in terms of the quantities measured which must include the ambient temperature.

$$V_\infty = \sqrt{2(p_t/p_\infty - 1)RT_\infty} \tag{13}$$

For Mach numbers above 0.5, it is advisable to use the compressible flow equivalent of Eq. (13)

$$V_\infty = \sqrt{2[\gamma/(\gamma-1)][(p_t/p_\infty)^{(\gamma-1)/\gamma} - 1]RT_\infty} \tag{14}$$

The velocity is seen to depend on the gas properties γ and R. Thus, it's measurement interacts with determination of atmospheric composition, or, alternatively, depends on the existence of relatively accurate estimates of γ and R. For accuracy, the data should be corrected also for vehicle attitude at the instant of measurement. Attitude is obtainable either from the accelerometers (see above) or from readings of symmetrically placed pressure orifices. In any case, these corrections are quite small for Mach numbers below 0.5.

Once velocity history is defined from entry to impact, it will provide the altitude as a function of time:

$$h = \int_t^{t_{impact}} (V_\infty \sin\theta)dt \tag{15}$$

The angle θ is the flight-path angle relative to horizontal, so that $V \sin\theta$ is the vertical component of velocity. Errors in altitude determination are minimized by use of vertical entry, $\theta = 90^\circ$. Errors in determining altitude will be discussed below.

With the above general features of the problem established, we now proceed to three special topics:

1. A very important interaction of the vehicle angular motion with the necessary data quantity.
2. A special gasdynamic problem of the spherical configuration.
3. Over-all accuracy of the profile of atmospheric density with altitude.

Effect of Vehicle Angular Motion on Necessary Data Quantity

The angular motion during entry of the atmospheric probe about its center of gravity depends on its initial attitude and angular rates about the three axes, as well as on the atmospheric properties and the gasdynamic stability of the probe.[13,14] Three typical motions are shown in Fig. 5: (a) a planar motion, obtained when the initial displacement and angular rate are confined to a single axis, (b) a damped circular precessing motion, obtained when the initial angular momentum is confined to the spin axis and there is an initial misalinement of that axis with the flight direction, (c) a more complicated gyroscopic motion, obtained when the initial angular momentum is not confined to the spin axis. The frequency of these motions for typical Mars entry conditions with small atmospheric probes is of the order of 5 to 10 cps at maximum dynamic pressure.

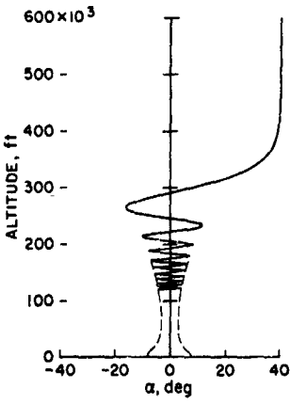

(a) Damped Planar Motion

Fig. 5 Typical Vehicle Angular Motions During Entry

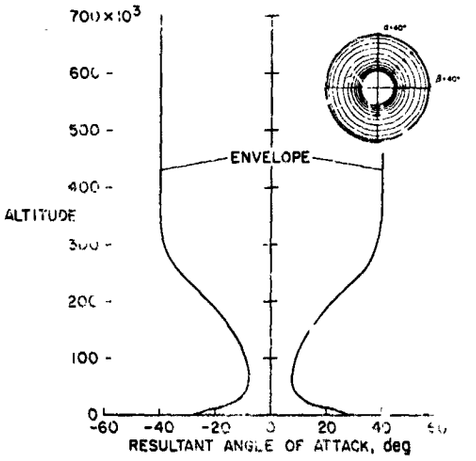

(b) Damped Precessing Circular Motion

Fig. 5 Continued

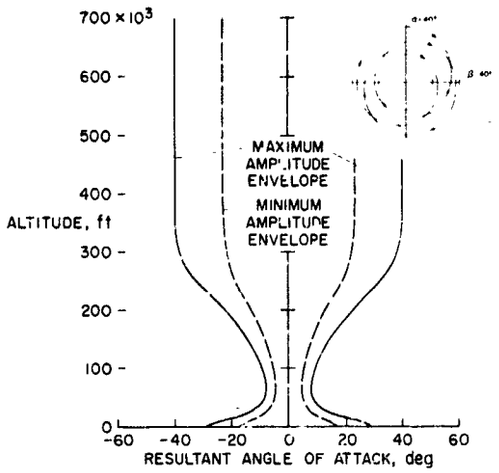

(c) More Complicated Gyroscopic Motion

Fig. 5 Concluded

Since the drag coefficient is in general a function of the attitude, it undergoes cyclic variations at twice the frequency of the attitude oscillations, and causes the drag acceleration to oscillate with time. The amplitude and frequency of the resulting oscillations in the acceleration history for the planar motion case of Fig. 5(a) are shown in Fig. 6. For the damped

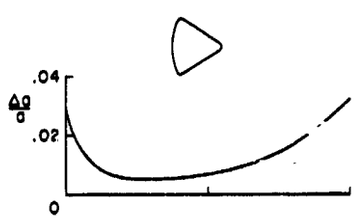

(a) Oscillatory Amplitude

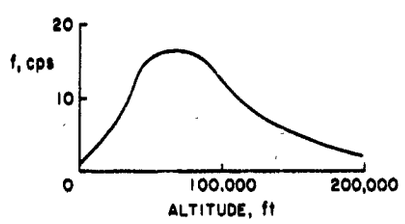

(b) Frequency

Fig. 6 Amplitude and Frequency of Oscillations in the Acceleration History for an Entry Vehicle Undergoing the Motion of Fig. 5(a)

circular precession, case 5(b), there would be no oscillating component, but a steady variation of drag coefficient with attitude as the motion becomes damped. The elliptical precession, case 5(c), is intermediate between the other two.

The accurate determination of velocity by integration of the accelerations requires that the oscillating acceleration pattern be defined, or, equivalently, that the amplitude pattern and frequency of angular motion be defined as functions to time. Randomly timed readings of the drag acceleration at intervals comparable to or longer than the period of oscillation can differ appreciably from the instantaneous mean value of acceleration, and seriously degrade the definition of velocity. To define the oscillating pattern requires, according to ballistic range experience, about three or four readings per cycle - e.g., with frequency of 16 cps, 50 readings per second. The disadvantage of this high data rate for missions where the communication is to be completed prior to impact[2] can be avoided in the following ways.

If the motion can be confined to the purely circular precession, the reading rate can be reduced to the minimum necessary to establish the smooth acceleration curve and the angular amplitude history, perhaps as few as two readings per second. To achieve this solution requires control over the initial conditions at entry, i.e., reduction of initial angular momentum about pitch and yaw axes to very small values compared to the spin momentum. This should be achievable by careful design of the probe release system.

The body of constant drag coefficient, independent of attitude, provides the second means of reducing the data rate. When the drag coefficient is constant, the oscillations in the acceleration disappear, and the reading rate can again be chosen on the basis of other considerations. The reduction of reading rate by an order of magnitude is, for communication at the distances of planetary missions, a sizable advantage and one certainly worth realizing by one or the other of these approaches.

A Gasdynamic Problem of the Sphere

The advantages of constant drag coefficient, independent of angle of attack, and zero or negligible lift-force development have been described. They are considerable, both for substantially reducing the total data communicated and for simplifying and making more precise the analysis of the atmospheric data. These considerations strongly suggest the use of an atmospheric probe of spherical shape, which possesses complete rotational symmetry and therefore has external aerodynamics fully independent of attitude.[15] The spherical probe considered has its mass offset forward, however, to maintain a given stable attitude so as to present the instrumentation, heat shield, and structure to the shock layer in a preferred rather than an uncontrolled fashion. It is assumed in this argument that such a sphere develops no steady lift force.

The assumption of zero lift is not, however, entirely supported by the observational data of which a considerable amount is available for spheres.[16,17] While much of this data is qualitative, the presence of a lift-generating mechanism is clear, at least for subsonic speeds and Reynolds numbers from about 50,000 to 200,000. One example of this is in the behavior of a nonspinning baseball, the so-called "knuckle ball," which is well known among ball players to exhibit very erratic flight patterns in its path to

the batter. Of course, the baseball is not perfectly smooth and symmetrical, having seams, but in light of the other evidence it seems likely that the cause of its erratic motion would be present for the smooth condition also, and we have referred to the lift production as the knuckle-ball effect. Similar erratic motion may be observed by dropping a ball bearing or marble in a water tank of sufficient depth, e.g., a swimming pool. Another example is the swerving motion exhibited by smooth weather balloons during ascent.

The lift production is attributable to unsymmetrical separation of the boundary layer from the sphere at stations near the maximum diameter where it leaves the body to form the wake. The pressure along the bounding streamline of the separated flow tends to assume the value on the body at the point of separation, so that differences in separation point on opposite sides of the body introduce differences in pressure distribution which lead to lift. The Reynclds number range in which the effect is normally observed is the laminar boundary layer regime, and little is known about whether it would be present with turbulent boundary layer, or whether it is an event connected with transition between the two. It may be that tripping the boundary layer with roughness would bring about the desired symmetry of flow and pressure distribution. These things are being studied at Ames Research Center. A shadowgraph showing asymmetrical separation is reproduced in Fig. 7(a).

(a) $M_\infty = 0.73$

Fig. 7 Shadowgraphs of Flow Separation on Sphere

At supersonic and hypersonic speeds, there is evidence to show that the lift production is zero or negligible. Greater symmetry is evidenced in flow separation patterns, Fig. 7(b). No measurable amount of swerve or erratic flight motion is detected in ballistic range tests, Fig. 8. Finally, and most convincing, data obtained on the density of the Earth's atmosphere from the deceleration of spherical bodies show very small scatter and good consistency at these speeds, deteriorating to show scatter at low speeds.[4] Hence, the problem seems to be asscciated with low speed flow only.

(b) $M_\infty = 2.8$

Fig. 7 Concluded

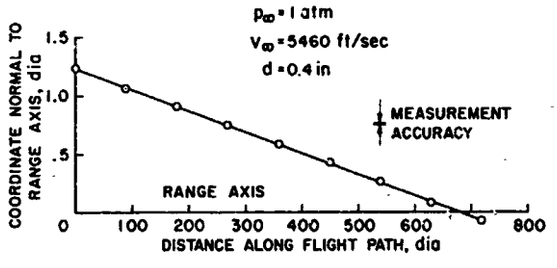

Fig. 8 Data Showing Straightness of Flight Path of a Sphere in Supersonic Flight

What is the implication of this effect for the planetary atmosphere experiments? It is clear that density data from accelerometers would be considerably degraded (with errors up to perhaps a factor of 2) by the presence of an unknown, fluctuating lift force if it were comparable in magnitude to the drag. It is also clear that error would be introduced into the integration of acceleration to track the velocity. However, if these effects are limited to subsonic speeds, they do not in fact cause problems, since the primary dependence at subsonic speeds is on direct measurement of static pressure and temperature and on velocity determination by airspeed indication or Doppler shift of the communication signal. Thus, if the fluctuating lift occurs only in this speed range, it does not degrade the data.

Work is in progress at Ames Research Center to test these conclusions, and to illuminate more fully the basic nature of the effect, if possible. This work includes free drops of spherical bodies from aircraft, with accelerometer and other instrumentation on board. In addition, we remain interested in other bodies which have C_L nearly independent of angle of attack, and small lift, such as the conical bodies referred to earlier. These configurations, while they do not possess perfectly the symmetry, constancy of C_D, and absence of systematic lift generation of the sphere, have the advantage of having a definite location of flow separation at the body base, and are thus free of the unsymmetrical separated flow effects that cause fluctuating lift.

Error Analysis

In the early portion of this paper techniques were described for determining the atmospheric structure (i.e., density and pressure as functions of altitude) using on-board measurements of deceleration, pitot pressure, static pressure, and ambient temperature. It is appropriate, at this point, to discuss the accuracy with which the atmospheric structure can be defined by these measurements. During the high speed portion of the entry, atmospheric density and pressure and entry vehicle altitude are determined from the vehicle deceleration. Errors in these quantities have been analyzed on the assumption that a bias error of a given fraction of the full-scale range exists in the accelerometer. Bias errors are emphasized because they are more instrumental in causing error in the density, pressure, and altitude than are random errors of the same magnitude. The latter tend to be averaged or cancelled out in the data smoothing.

The effect of accelerometer bias on density, pressure, velocity, and altitude can be determined by taking the partial derivative with respect to acceleration of the expressions for those quantities as given in Eqs. (5), (6), (11), and (15). It is convenient to express the resulting errors in density and pressure as fractions of the values of density and pressure. The resulting expressions for errors due to accelerometer bias have been determined under the assumption that flight-path angle, θ, is constant during the entry, and are given by:

$$\left(\frac{\Delta\rho}{\rho}\right)_{\Delta a} = \left(\frac{1}{a_s} + \frac{2t}{V}\right)\Delta a \qquad (16)$$

$$\left(\frac{\Delta p}{p}\right)_{\Delta a} = \frac{\int_o^t \left(\frac{V + a s t}{V^2}\right) dt}{\int_o^t \frac{a_s}{V}\, dt} \Delta a \qquad (17)$$

$$\Delta h_{\Delta a} = - \frac{t^2_{impact} - t^2}{2} \sin\theta \, \Delta a \qquad (18)$$

These errors due to an accelerometer bias of 0.1 percent of the maximum deceleration measured are shown as a function of velocity in Fig. 9. A

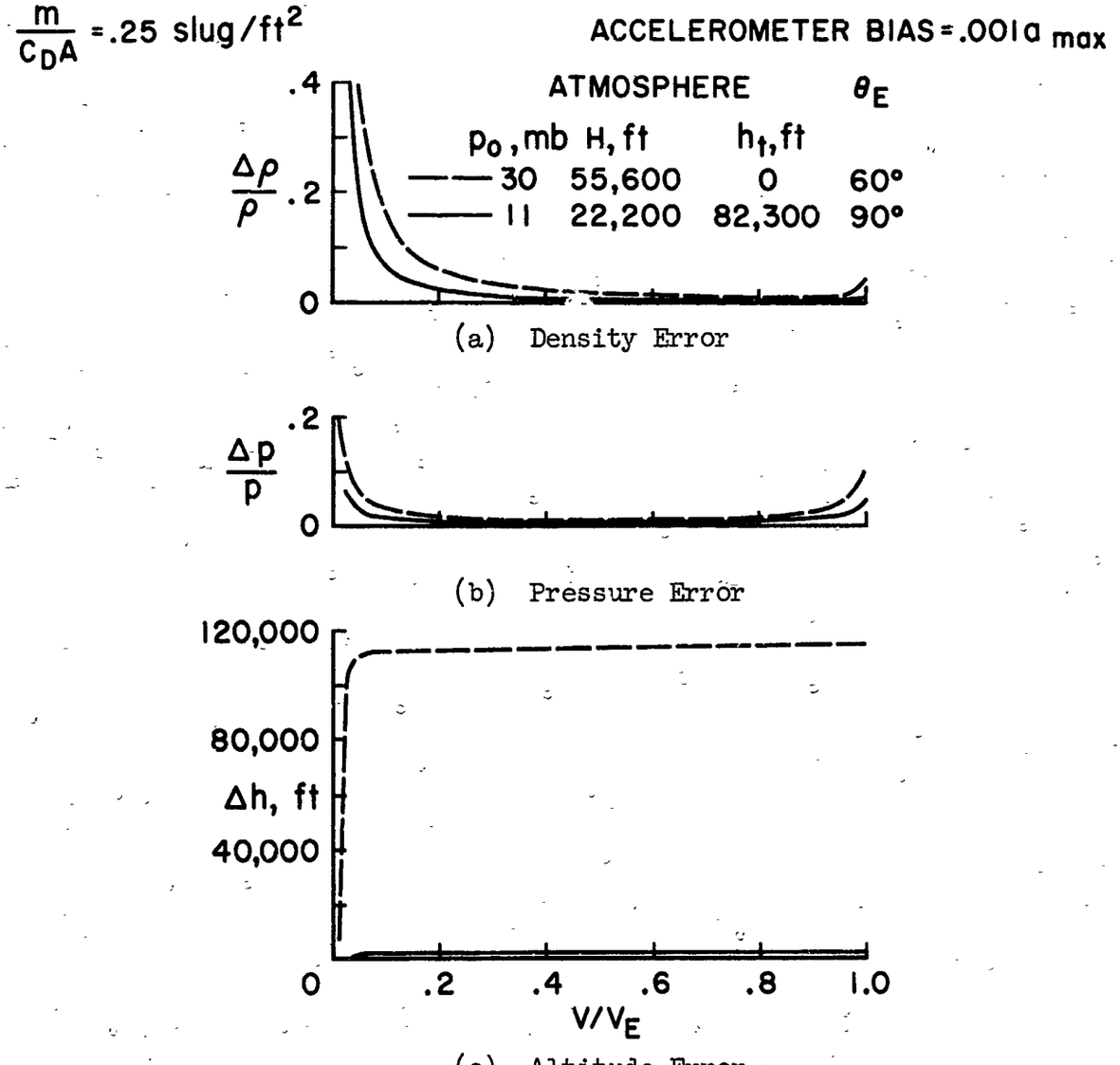

Fig. 9 Errors in Atmospheric Structure Determination Due to Accelerometer Bias

vertical entry into a small scale height atmosphere and a 60° entry into a large scale height atmosphere were chosen to illustrate the range of errors to be expected from this source. Note that density and pressure are determined within 6 percent over virtually the entire velocity range down to 0.2 V_E. The altitude determination for entry into the low scale height atmosphere is excellent; that for the large scale height, however, is in serious error. This is the result of the long time spent at low speeds where the velocity, and hence the altitude, determination given by the accelerometers is poor. Since errors in altitude are, in a sense, equivalent to errors in density or pressure, the error in altitude shown for the large scale height atmosphere is considered unacceptable and the additional measurements discussed earlier are necessary in the low speed portion of the entry.

From the measurements during subsonic flight of pitot and static pressure and ambient temperatures, the density may be calculated from the equation of state (eq. (7)). Inspection of this equation shows that fractional errors in density will be equal to fractional errors in pressure, temperature, and gas constant (in the small error range). Sources of error in the determination of subsonic velocity, and hence altitude, will, in addition, include that due to uncertainty in specific heat ratio, γ. Expressions for the error in altitude can be derived by taking the partial derivative of Eq. (14) with respect to the quantity in question and substituting the result in the following equation for altitude error:

$$\Delta h = \int_{t}^{t_{impact}} \Delta V \sin\theta \, dt \tag{19}$$

The resulting expressions for error in altitude due to the various sources are as follows:

$$\Delta h_{\Delta R} = \frac{1}{2}\frac{\Delta R}{R} h \tag{20}$$

$$\Delta h_{\Delta T} = \frac{1}{2}\frac{\Delta T}{T} h \tag{21}$$

$$\Delta h_{\Delta \gamma} = \frac{1}{2}\frac{\Delta \gamma}{\gamma}\int_{t}^{t_{impact}} \left[\frac{1}{\gamma} \frac{(p_t/p)^{\frac{\gamma-1}{\gamma}} \ln(p_t/p)}{(p_t/p)^{\frac{\gamma-1}{\gamma}} - 1} - \frac{1}{\gamma - 1} \right] V \sin\theta \, dt \tag{22}$$

$$\Delta h_{\Delta p_t} = \int_{t}^{t_{impact}} \left(\frac{p_t}{p}\right)^{\frac{\gamma-1}{\gamma}} \frac{\Delta p_t}{p_t} V \sin\theta \, dt \tag{23}$$

$$\Delta h_{\Delta p} = -\int_{t}^{t_{impact}} \left(\frac{p_t}{p}\right)^{\frac{\gamma-1}{\gamma}} \frac{\Delta p}{p} V \sin\theta \, dt \tag{24}$$

Root-sum-square errors in pressure, density, and altitude due to pressure and temperature sensor bias of 1 percent and 5 percent, respectively, and uncertainties in specific heat ratio and gas constant of 5 percent and 10 percent, respectively, are shown in Fig. 10 as a function of velocity from sonic

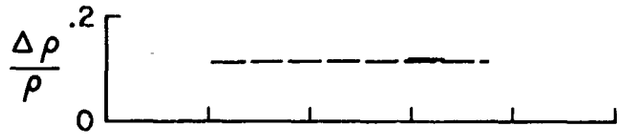

(a) Density Error

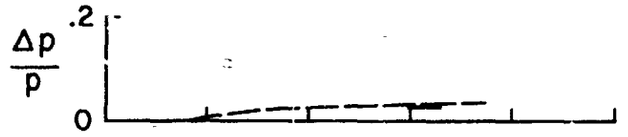

(b) Pressure Error

$m/C_DA = .25$ slug/ft^2
PRESSURE BIAS = .01 p_{max}
TEMPERATURE BIAS = .05 T_{max}
SPECIFIC HEAT RATIO UNCERTAINTY = .05γ
GAS CONSTANT UNCERTAINTY = .10R

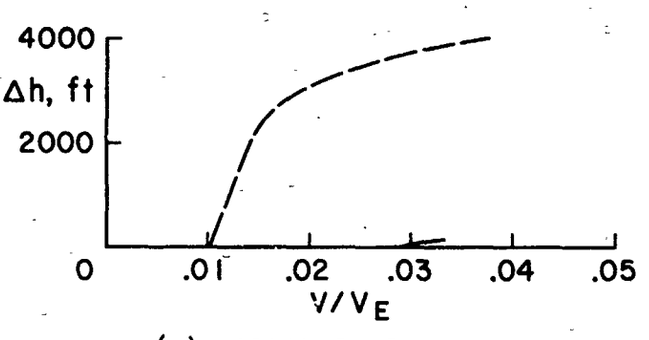

(c) Altitude Error

ATMOSPHERE			θ_E
p_0, mb	H, ft	h_f, ft	
30	55,600	0	60°
11	22,200	82,300	90°

Fig. 10 Errors in Atmospheric Structure Determination at Low Speed Due to Errors in Pressure, Temperature, Specific Heat Ratio, and Gas Constant

speed to impact speed. Note that the maximum error in altitude for entry into the large scale height atmosphere is only 4,000 feet from this source, whereas the error, over the same velocity range, due to accelerometer bias is 110,000 feet.

Uncertainty in entry velocity and flight-path angle will also affect the accuracy of the results. However, studies of the guidance and tracking capabilities of existing systems for interplanetary vehicles, as well as the maneuver required to separate the entry vehicle from the bus and place it on an impact trajectory with the planet, indicate that entry velocity will be known within a few feet per second and entry flight-path angle within a few degrees.

As a test of the over-all definition of atmospheric density structure that might be achieved, analysis has been made including all of the factors discussed above. The results of these calculations are shown in Fig. 11 where

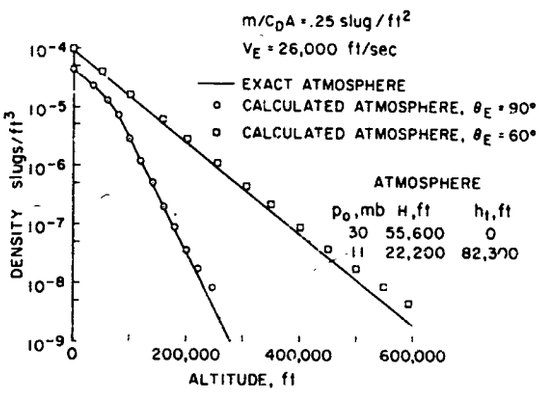

Fig. 11 Over-all Accuracy of Atmospheric Density Profile

the calculated density profiles are represented by the symbols and are compared with the "exact" atmospheres postulated. The definition is excellent from ground level to the altitudes where the vehicle is first able to sense the atmosphere, which occurs at density levels of 10^{-5} of Earth sea-level density.

The technique of determining atmospheric density by deceleration measurements on a spherical entry vehicle has been used with considerable success by the University of Michigan[3] and the Air Force Cambridge Research Laboratories[4] in the determination of Earth atmosphere density. In this case data were obtained by ejecting a small (7-inch diameter) metal sphere from a sounding rocket at an altitude about 60 km. The spheres coasted up to maximum altitudes near 200 km and measurements were made on both the upward and downward legs of the trajectory. Results typical of these measurements are shown in Fig. 12 which is reproduced from Ref. 4. The high quality of these results is apparent and is evidence not only of the efficacy of the technique but also of the high quality of work and attention to detail that the Air Force Cambridge Research Laboratories invested in the measurements.

DETECTION OF CHEMICAL SPECIES IN THE SHOCK LAYER BY SPECTROMETRY

The atmospheric gases which pass through the bow wave of the entry body into the shock layer are heated by shock compression to a very high temperature at which molecular rotation and vibration and electronic energies above the ground state are excited with consequent radiative emission in transitions to lower energy states. The characteristic wavelengths and intensities emitted can be used to identify and determine number densities of the emitting species in the shock layer. On the assumption that Mars' atmosphere is composed largely of nitrogen and carbon dioxide, a considerable amount of laboratory work and theoretical calculation has been performed to study the radiative emissions of this type from these gas mixtures.[18-21] Use will be made of

these studies to show the potentialities of shock layer spectrometry for quantitatively detecting the presence of selected atmospheric constituents.

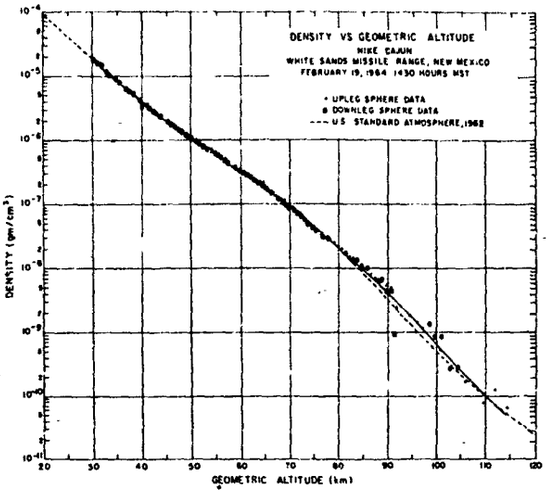

Fig. 12 Earth Atmosphere Density Profile as Determined by the Sphere Deceleration Measurements of Ref. 4

Compared to the spectroscopic study of radiation from some other sources, the measurement of shock layer radiation has one significant advantage which should be pointed out. The state of the gas behind the shock wave at equilibrium may be calculated exactly by use of the well-known Rankine-Hugoniot equations for any given atmosphere, density, and shock-wave velocity. Examples of such calculations are given in Ref. 22. This capability makes it possible not only to predict the spectral distribution for hypothetical atmospheres and trajectories, but also to analyze quantitatively the spectrometer data for those cases where the shock layer may be assumed to be in equilibrium.

To better appreciate the nature of the shock compression process, consider as an example a blunt body such as the sphere shown in the sketch preceded by a

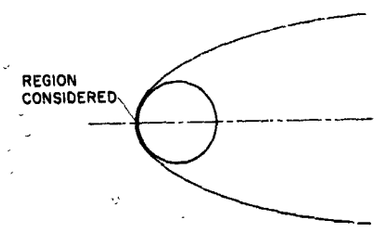

Sketch (b)

shock wave (which is normal to the flow on the wave axis of symmetry) at a velocity of 20,000 ft/sec in an atmosphere having a pressure of 0.01 of Earth sea-level atmospheric pressure and a composition of 0.25 CO_2 and 0.75 N_2. Behind the normal shock wave at equilibrium, according to theory,[22] the pressure is 440 times greater than ambient, the temperature is approximately 6750° K, and the gas has undergone the chemical rearrangement indicated in Fig. 13. The carbon dioxide has all but disappeared, being replaced by dissociation products CO and C; the nitrogen is partially dissociated; and some

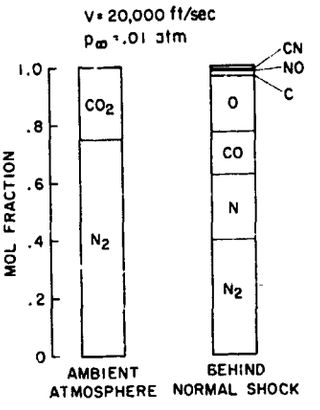

Fig. 13 Typical Composition of Gas in Shock Layer for Nitrogen-Carbon Dioxide Atmosphere at Mars Entry Velocity

new species CN and NO resulting from high temperature reactions are present in amounts of about 1 percent. Since this chemical rearrangement is a predictable consequence of the shock compression, it does not detract from the possibility of determining the free-stream gases by observation of those in the shock layer, except that other mixtures having the same proportions of the same atoms in the free stream would perhaps be difficult to distinguish from the given mixture of nitrogen and carbon dioxide, e.g., mixtures containing NO and CO in the free stream. The nonequilibrium zone which exists immediately behind the bow wave may, however, aid in making this distinction.

Given the equilibrium composition and the calculable equilibrium distribution of the various species over their energy states, one needs in addition the transition probabilities for the radiative reactions to obtain theoretically the equilibrium radiative emission to be expected. The transition probabilities have been determined in the laboratory for the radiative processes which must be considered here (see, e.g., Refs. 23 and 24), and a theoretical spectrum for the mixture discussed above is presented in Fig. 14, taken from the calculations of Ref. 21. To avoid confusion, the data for different band systems are presented on separate levels of the graph and with different scales. The CN radical, while present in small amounts, has, by far the brightest emission, the CN violet system. To observe this bright band system on Mars would constitute direct evidence of nitrogen in the atmosphere, which is thus far only speculation, and, as will be shown, measurement of the intensity of the band will yield information on the mole fraction of nitrogen in the atmosphere.

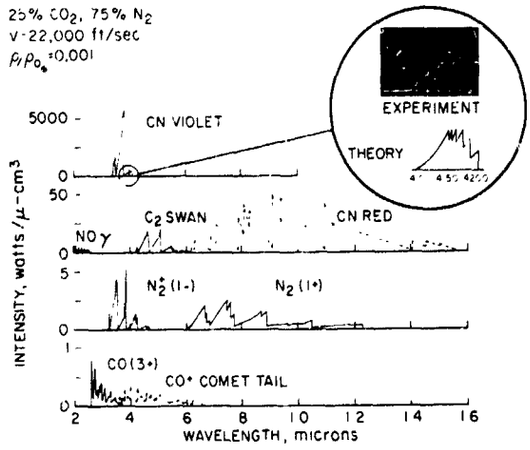

Fig. 14 Calculated Shock Layer Spectra

These theoretical results have been found to be generally well supported by experiments in which small scale models are gun-launched in free flight through selected gas mixtures and the shock layer radiation measured by stationary radiometers at a station along the flight path.[21] Three comparisons of experiment and theory are of sufficient interest and pertinence to be included here. The first, Fig. 15, shows the theoretical mole fraction of CN in the shock layer compared with the experimental luminous intensity of the CN violet bands, plotted as a function of the fraction of CO_2 in the atmospheric gas mixture where the remainder is nitrogen. In mixtures ranging from pure nitrogen to pure carbon dioxide, the luminous intensity is found to vary in proportion to the quantity of CN in the shock layer. The data were taken from Ref. 18, the mole fractions of CN from Ref. 22.

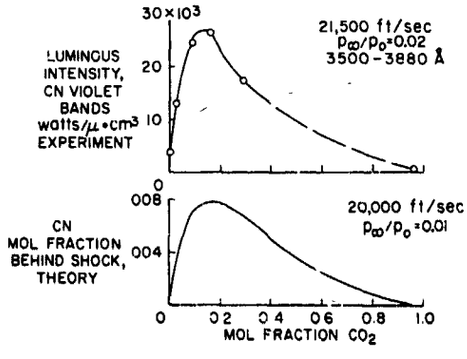

Fig. 15 Mixture Dependence of CN Violet Radiation

Two observations obtained by Ellis Whiting of Ames Research Center supply absolute evidence of the identity of the CN violet bands in the shock layer. One, included as an inset of Fig. 14, is an oscilloscope record of the output of a sweeping monochromator with a resolution of about 15Å of the radiation from the shock layer between 4100 and 4200Å. The theory for the corresponding CN violet side band is reproduced under the oscilloscope trace, and has, within the limits of the resolution, unmistakably the same detailed features as the experiment. The second observation, a photographic spectrum is reproduced in Fig. 16. This picture, obtained as the shock layer of a small model flew past the entrance slit of the spectrograph, had an exposure time of less than a microsecond, but this was sufficient to record the CN violet system. None of the other spectral features was bright enough to expose.

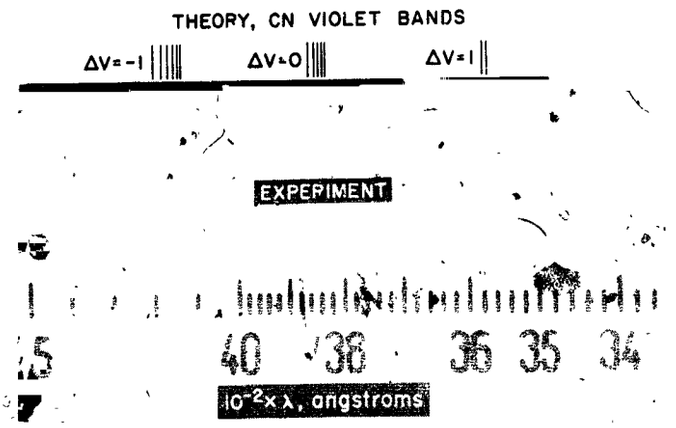

Fig. 16 Photographic Spectrum of Radiation From the Shock Layer of a Model Flying at a Velocity of 21,100 ft/sec in a 0.09 CO_2 - 0.91 N_2 Mixture

Figure 15 shows that for mixtures of nitrogen and carbon dioxide, a measurement of the luminous intensity will identify the mole fraction of carbon dioxide as being one of two possible values. A record of the band intensity as a function of velocity along the entry trajectory will resolve which of these two values is correct, as shown in Fig. 17. The 9-percent and 25-percent carbon dioxide mixtures have the same emission at about 19,000 ft/sec, but at other velocities differ by sizable factors. Plotting such an experimental trace and comparing it with theoretical traces for various mixture ratios would permit the identification of the atmospheric mixture proportions.

If nitrogen is absent from the atmosphere, or if other gases are important constituents, much can still be learned from the spectrometric experiment. The demonstration that nitrogen is not a major atmospheric constituent would be in itself a valuable negative result. Other gases likely to be constituents include argon and nitrogen oxides. With nitrogen oxides, the increased ratio of oxygen to nitrogen atoms in the shock layer will enhance the mole fraction of NO at equilibrium, and a detector to observe the NO gamma band system would permit the observation of this enhancement. The addition of argon increases the shock layer temperature at a given flight velocity. The temperature can be measured spectroscopically, but whether this would be an accurate

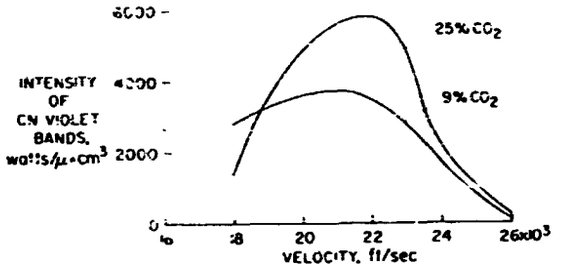

Fig. 17 Trajectory Dependence of CN Violet Radiation

enough indication of the mole fraction of argon remains to be determined. Equally promising is the shift to lower velocities in the peak of the CN violet band intensity due to the addition of argon,[19] again an effect of increased temperature. Thus, by determination of the ratio of N_2/CO_2 and the velocity for peak emission, the mole fraction of argon may be defined. Also not to be overlooked is the direct observation of a bright argon line with a narrow band detector. Some of these techniques will require further detailed study.

The effects of nonequilibrium chemistry and thermodynamics behind the shock wave will be important for some conditions. The introduction of nonequilibrium processes forces an increased dependence on laboratory experiments to replace theory for interpretation of the data. Such experiments can be performed in shock tubes with both the density and velocity conditions of flight duplicated. This permits the study in detail of the spatial variation of radiation behind the wave. Measurements of this kind reported in Ref. 20 as well as those in Ref. 21 show that the spectral distribution of radiation is very much the same for equilibrium and nonequilibrium regions, i.e., the principal radiators are the same. The fact that such laboratory facilities exist to duplicate the conditions and provide experimental assistance in the interpretation of the data, both before and after the flight test, is of great value in the conduct of such planetary experiments.

CONCLUDING REMARKS

The detailed studies which have been described were intended to indicate the feasibility and the promise of experiments making use of entry probe responses to define the structural and compositional features of the Mars' atmosphere. As with any undertaking of measurements of other than the most elementary nature, numerous features are found which require thoughtful and detailed consideration and demand correctness of approach in order for the experiments to succeed. However, no features have been found which would prevent the successful measurement of the Mars' atmosphere, or that of other planets, by these

techniques, and the information obtained would be most valuable, and, in some respects, difficult to obtain by other techniques. Further efforts are being applied to treat questions which may still exist.

NOTATION

a	acceleration
A	frontal area
c_p	specific heat at constant pressure
C_D	drag coefficient
C_F	resultant force coefficient
C_{L_α}	lift-curve slope
d	body diameter
D	drag force
f	frequency
F	resultant gasdynamic force
g	acceleration due to gravity
h	altitude
$\overline{h}$	gas enthalpy
h_t	tropopause altitude
H	atmospheric scale height
L	lift force
m	entry probe mass
M	Mach number
p	pressure
p_t	pitot pressure
P	pressure coefficient
q	dynamic pressure
R	gas constant
Re	Reynolds number
t	time
T	gas temperature
V	velocity
x	coordinate along body axis
X	gasdynamic force along body axis
y	coordinate normal to body axis
Y	gasdynamic force normal to body axis

α angle of attack

β angle of sideslip

δ flow deflection angle at body surface

Δ increment due to error or to oscillation

γ ratio of specific heats of atmospheric gases

λ wavelength

φ $\tan^{-1} L/D$

ρ gas density

θ flight-path angle below horizontal

Subscripts

o zero altitude

d based on diameter

E entry into the atmosphere

l based on length

s in flight direction

x along body axis

y normal to body axis

∞ ambient atmosphere

REFERENCES

1. A. Seiff, Some Possibilities for Determining the Characteristics of the Atmospheres on Mars and Venus From Gas-Dynamic Behavior of a Probe Vehicle, NASA TN D-1770, 1963.

2. A. Seiff and D. E. Reese, Jr., "Definition of Mars' Atmosphere, a Goal for the Early Missions," Astronautics and Aeronautics, Feb. 1965.

3. L. M. Jones, J. W. Peterson, E. J. Schaefer, and H. F. Schulte, "Upper-Air Density and Temperature: Some Variations and an Abrupt Warming in the Mesosphere," J. Geophys. Res., vol. 64, No. 12, Dec. 1959, pp. 2331-40.

4. K. S. W. Champion and A. C. Faire, Falling Sphere Measurements of Atmospheric Density, Temperature, and Pressure, up to 115 km, AFCRL-64 554, Air Force Cambridge Res. Lab., July 1964.

5. C. M. Sabin, The Effects of Reynolds Number, Mach Number, Spin Rate, and Other Variables on the Aerodynamics of Spheres at Subsonic and Transonic Velocities, BRL Memo Rep. 1044, Nov. 1956.

6. R. Lehnert, Base Pressure of Spheres at Supersonic Speeds, Navord Rep. 2774, U.S. Naval Ordnance Lab., White Oak, Maryland, Feb. 1953.

7. A. J. Hodges, "The Drag Coefficient of Very High Velocity Spheres," J. Aero. Sci., vol. 24, No. 10, Oct. 1957, pp. 755-8.

8. A. Seiff and S. C. Sommer, An Investigation of Some Effects of Mach Number and Air Temperature on the Hypersonic Flow Over a Blunt Body, NASA MEMO 10-9-58A, 1959.

9. A. Seiff, S. C. Sommer, and T. N. Canning, Some Experiments at High Supersonic Speeds on the Aerodynamic and Boundary-Layer Transition Characteristics of High-Drag Bodies of Revolution, NACA RM A56I05, 1957.

10. A. Seiff, "Atmosphere Entry Problems of Manned Interplanetary Flight," AIAA Conf. Engineering Problems of Manned Interplanetary Exploration, Palo Alto, Calif., Sept. 30-Oct. 1, 1963. AIAA, New York, 1963, pp. 19-33.

11. G. P. Menees and W. G. Smith, A Study of the Stability and Drag of Several Aerodynamic Shapes in Air, Carbon Dioxide, and Argon at Mach Numbers From 3 to 8, NASA TM X-950, 1964.

12. F. S. Holman and H. Kennet, "Planetary Atmospheric Determination Utilizing a Semipassive Probe," The Boeing Co., June 1964.

13. H. J. Allen, Motion of a Ballistic Missile Angularly Misaligned With the Flight Path Upon Entering the Atmosphere and Its Effect Upon Aerodynamic Heating, Aerodynamic Loads, and Miss Distance, NACA RM A56F15, 1956.

14. M. Tobak and V. L. Peterson, Angle-of-Attack Convergence of Spinning Bodies Entering Planetary Atmospheres at Large Inclinations to the Flight Path, NASA TR P-210, 1964.

15. V. L. Peterson, A Technique for Determining Planetary Atmosphere Structure From Measured Acceleration of an Entry Vehicle, NASA TN D-2609, 1965.

16. E. Jacobs, "Experimental Methods -- Wind Tunnels, Part 2," Publ. as a part of vol. III of Aerodynamic Theory, W. F. Durand, Editor, Berlin, Springer, 1934-6, pp. 323, 328, and 329.

17. Anon.,"Spiraling Spheres," in Science and the Citizen, Scientific American, vol. 210, No. 2, Feb. 1964, pp. 71-72.

18. C. S. James, "Experimental Study of Radiative Transport From Hot Gases Simulating in Composition the Atmospheres of Mars and Venus," AIAA Conf. Physics of Entry Into Planetary Atmospheres, Aug. 26-28, 1963, Massachusetts Institute of Technology, Cambridge, Mass. AIAA Paper 63-455.

19. F. Wolf and T. Horton, "Effect of Argon Addition on Shock-Layer Radiance of CO_2-N_2 Gas Mixtures," AIAA J., vol. 2, No. 8, Aug. 1964, pp. 1472-74.

20. G. M. Thomas and W. A. Menard, "Experimental Measurements of Non-equilibrium and Equilibrium Radiation From Planetary Atmospheres," AIAA Entry Tech. Conf., Williamsburg and Hampton, Va., Oct. 12-14, 1964. AIAA, New York, 1964, pp. 170-85.

21. J. O. Arnold, V. H. Reis, and H. T. Woodward, "Theoretical and Experimental Studies of Equilibrium and Nonequilibrium Radiation to Bodies Entering Postulated Martian and Venusian Atmospheres at High Speeds," AIAA Second Aerospace Sciences Meeting, New York, N. Y., Jan. 1965. AIAA Paper 65-116.

22. H. T. Woodward, Thermodynamic Properties of Carbon-Dioxide and Nitrogen Mixtures Behind a Normal Shock Wave, NASA TN D-1553, 1963.

23. V. H. Reis, "Oscillator Strengths for the N_2 Second Positive and N_2^+ First Negative Systems From Observations of Shock Layers About Hypersonic Projectiles," J. Quantitative Spectroscopy and Radiative Transfer, vol. 4, No. 6, 1964, p. 783.

24. R. G. Bennett and F. W. Dalby, "Experimental Determination of the Oscillator Strength of the First Negative Bands of N_2^+, J. Chem. Phys., vol. 31, No. 2, Aug. 1959, pp. 434-41.